5790 *Biochemistry* **2010,** *49,* 5790–5798
DOI: 10.1021/bi100690k

BIOCHEMISTRY
including biophysical chemistry & molecular biology
Article

Potent and Selective Inhibition of the Open-Channel Conformation of AMPA Receptors by an RNA Aptamer[†]

Zhen Huang, Yan Han, Congzhou Wang, and Li Niu*

Department of Chemistry and Center for Neuroscience Research, University at Albany, State University of New York, Albany, New York 12222

Received May 4, 2010; Revised Manuscript Received June 1, 2010

ABSTRACT: Inhibitors of AMPA receptors are useful as biochemical probes for structure−function studies and as drug candidates for a number of neurological disorders and diseases. Here we report the identification of an RNA inhibitor or aptamer by an in vitro evolution approach. Using a laser-pulse photolysis technique, we further characterized the mechanism of inhibition of this aptamer on the AMPA receptor channel-opening rate process in the microsecond-to-millisecond time domain. Our results show that the aptamer we isolated is a noncompetitive inhibitor that selectively inhibits the open-channel conformation of AMPA receptors with nanomolar affinity. The potency and the selectivity of this noncompetitive aptamer rival those of small molecule inhibitors. Our results therefore demonstrate the utility of this approach in developing water-soluble, highly potent, and conformation-selective noncompetitive inhibitors of AMPA receptors.

A protein is generally dynamic and adapts a specific conformation for function (*1*, *2*). Using molecular agents that bind selectively to a specific protein conformation among its conformational repertoire is thus a powerful means of exerting a tighter molecular recognition to more effectively regulate the function of that protein, and to even engineer a new protein function. For instance, small chemical compounds have been found to stabilize a conformation for some apoptotic procaspases to induce autoproteolytic activation of these proenzymes (*3*). Catalytic antibodies have been created, on the basis of transition-state structural analogues, to accelerate chemical reactions by stabilizing their rate-determining transition states along reaction pathways (*4*).

Here we describe the discovery of RNA inhibitors or aptamers that selectively target the open-channel conformation of α-amino-3-hydroxy-5-methyl-4-isoxazolepropionic acid-subtype glutamate ion-channel receptors. The open-channel conformation exists on a time span of microseconds to a few milliseconds (*5*), after the receptors bind to glutamate, the endogenous neurotransmitter; even on the millisecond time scale, the glutamate-bound receptors turn into the desensitized, closed-channel receptor form (*6*). Only through the transient, open-channel conformation of the postsynaptic receptors is a nerve impulse transmitted in the central nervous system. AMPA[1] receptors are indispensible for brain development and activity such as memory and learning (*7*−*10*), whereas excessive activation of AMPA receptors, which leads to an intracellular calcium overload, has been implicated in various neurological diseases, such as cerebral ischemia and amyotrophic lateral sclerosis (*11*). Developing inhibitors to control excessive receptor activity is a long-pursued therapeutic strategy for a potential treatment of these neurological disorders and diseases.

To find inhibitors selectively targeting the open-channel conformation of AMPA receptors, we did not take the commonly used approaches, such as structure-based inhibitor design or organic synthesis of small molecules. There has been no structural information available for sites of noncompetitive inhibitors on AMPA receptors. There has not been any type of structural template, synthetic or natural products alike, that could have served as a template for developing a conformation-selective inhibitor of AMPA receptors. Because of these limitations, we decided to use an in vitro evolution approach, known as systematic evolution of ligands by exponential enrichment (SELEX), to identify potential RNA inhibitors or aptamers from an RNA library comprised of $\sim 10^{15}$ randomized sequences (*12*, *13*). This approach enables one to identify a desired RNA molecule(s) with a defined property against the target without preexisting templates (*14*), a concept and practice different from organic synthesis, the most commonly used approach for developing inhibitors and drugs (*15*, *16*). RNA aptamers can fold into potentially useful three-dimensional structures and can be identified using an in vitro elution approach to recognize virtually any target molecules as well as perform desired functions with high affinity and selectivity not found in nature (*17*). Using this in vitro evolution approach, we have indeed found an aptamer, described below, that potently and selectively inhibits AMPA receptors by targeting uniquely the open-channel conformation.

EXPERIMENTAL PROCEDURES

Cell Culture and Transient Receptor Expression. The original cDNAs encoding rat GluA1, -2, and -3 AMPA receptors and GluK2 kainate receptor were kindly provided by S. Heinemann. The GluA4 DNA plasmid was kindly provided by P. Seeburg. The GluK1 plasmid was kindly provided by G. Swanson. The cDNAs of all three *N*-methyl-D-aspartic acid (NMDA) receptor subunits were

[†]This work was funded in part by grants from the U.S. Department of Defense (W81XWH-04-1-0106) (to L.N.), the National Institutes of Health (R01 NS060812) (to L.N.), and the Muscular Dystrophy Association (to L.N.) and a postdoctoral fellowship from the Muscular Dystrophy Association (to Z.H.).

*To whom correspondence should be addressed. E-mail: lniu@albany.edu. Phone: (518) 591-8819. Fax: (518) 442-3462.

[1]Abbreviations: AMPA, α-amino-3-hydroxy-5-methyl-4-isoxazolepropionic acid; cpm, counts per min; HEK-293, human embryonic kidney; NMDA, *N*-methyl-D-aspartic acid; nt, nucleotide; SELEX, systematic evolution of ligands by exponential enrichment.

 Published on Web 06/02/2010

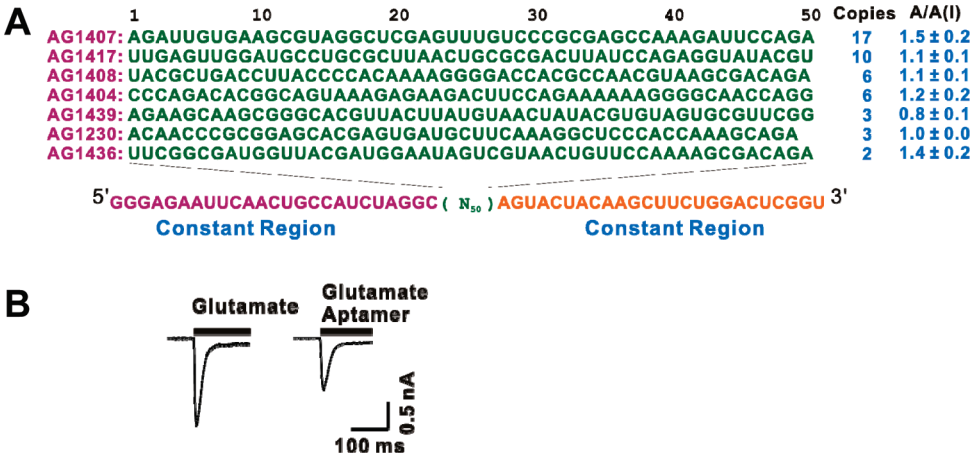

FIGURE 1: Enriched RNA sequences and their biological functions. (A) The seven enriched sequences are shown with their names at the left and copy numbers at the right, which represent the number of appearances of the same sequence in the entire sequence pool [83 sequences (see the text)]. The variable sequence region (N50) or the selected sequences are colored green, whereas the 5′ and 3′ constant regions are displayed at the bottom. The putative inhibition of GluA2Q$_{flip}$, the SELEX target, by these RNAs, as tested by whole-cell recording, is shown, on the right, as the ratio of the whole-cell current amplitude in the absence and presence of 500 nM aptamer or A/A(I) at 3 mM glutamate. (B) Representative traces of the whole-cell current response of GluA2Q$_{flip}$ to 3 mM glutamate in the presence of 500 nM AG1407. The current was recorded at −60 mV, pH 7.4, and room temperature with the same HEK-293 cell expressing GluA2Q$_{flip}$.

kindly provided by J. Woodward. All of the receptors were transiently expressed in human embryonic kidney (HEK-293S) cells. HEK-293S cells were maintained in Dulbecco's modified Eagle's medium supplemented with 10% fetal bovine serum and 1% penicillin in a 37 °C, 5% CO_2, humidified incubator. The DNA plasmids encoding green fluorescent protein and large T-antigen were cotransfected in HEK-293S cells (*18*). Transfected cells were used for recording 48 h after transfection. For the in vitro selection, the transfected cells were harvested 48 h after transfection, and the membrane fragment that contained the GluA2Q$_{flip}$ receptor was prepared as described previously (*19*).

In Vitro Selection. The preparation of the RNA library and the protocol of running the in vitro evolution selection were described previously (*19*) (Figure S1 of the Supporting Information). For binding in the initial round of selection, the RNA library with ~10^{15} random sequences was dissolved in the extracellular buffer, which contained 150 mM NaCl, 3 mM KCl, 1 mM $CaCl_2$, 1 mM $MgCl_2$, and 10 mM HEPES (pH 7.4). The final concentration of membrane-bound receptor in the binding mix was 8 nM, as determined by [^{3}H]AMPA binding. To keep the homomeric GluA2Q$_{flip}$ ion channels in the open-channel conformation, the membrane-bound receptor was exposed to 1 mM (final concentration) kainate for 5 min before being mixed with the RNA library. The mixture of the RNA library and the receptor was incubated at 22 °C for 50 min for RNA binding to the receptor in the presence of 0.3 unit/μL RNase inhibitor. For elution, we used 1 mM (final concentration) GYKI 47409. The eluted RNAs were then subject to reverse transcription-polymerase chain reaction (RT-PCR) (Figure S1 of the Supporting Information). At the end of the 14th selection round, the DNA pools from rounds 12 and 14 were separately cloned into the pGEM-T easy vector (Invitrogen) for sequencing. By sequence comparison, the enriched sequences were identified (Figure 1A) and tested functionally, described below.

Homologous Competitive Binding Assay. The 5′-end ^{32}P-labeled aptamer was first prepared as described previously (*19*). Then, 1 μL of 10 nM ^{32}P-labeled aptamer was mixed with 2 μg of yeast tRNA (Sigma) and a series of concentrations (i.e., 0−400 nM, final) of unlabeled (cold) aptamer. For receptor preparation, 4 fmol of the membrane-bound GluA2Q$_{flip}$ was suspended in the extracellular buffer with and without 1 mM kainate. The final concentrations for the receptor and for the hot aptamer, after mixing, were 0.4 and 0.1 nM, respectively. The mixture was incubated at 22 °C for 1 h for binding. The mixture was loaded onto a presoaked 0.45 μm nylon filter (VWR), which was then centrifuged at 4000 rpm for 5 min. The filter was washed twice with 400 μL of the extracellular buffer. The radioactivity on the filter was quantified in a scintillation counter (Beckman LS6500). The analysis of the homologous competition binding data (*20*) is described in detail in the Appendix.

Whole-Cell Current Recording. The procedure for whole-cell current recording to assay the inhibitory property of an RNA aptamer was previously described (*19*). The electrode for whole-cell recording had a resistance of ~3 MΩ, when filled with the electrode solution [110 mM CsF, 30 mM CsCl, 4 mM NaCl, 0.5 mM $CaCl_2$, 5 mM EGTA, and 10 mM HEPES (pH 7.4, adjusted with CsOH)]. The extracellular buffer composition is provided in In Vitro Selection. For recording of the NMDA channels, the intracellular solution contained 140 mM CsCl, 1 mM $MgCl_2$, 0.1 mM EGTA, and 10 mM HEPES [pH 7.2, adjusted with $Mg(OH)_2$], while the extracellular solution contained 135 mM NaCl, 5.4 mM KCl, 1.8 mM $CaCl_2$, 10 mM glucose, and 5 mM HEPES (pH 7.2, adjusted with NaOH). In the extracellular buffer, 100 μM glycine was added (*19*). All reagents including aptamer were dissolved in the corresponding extracellular buffer and used. All RNA samples were transcribed and purified as described previously (*19*). The glutamate-induced whole-cell current was recorded using an Axopatch-200B amplifier at a cutoff frequency of 2−20 kHz by a built-in, eight-pole Bessel filter and digitized at a sampling frequency of 5−50 kHz using a Digidata 1322A instrument from Axon Instruments (Molecular Devices, Sunnyvale, CA). pClamp 8 (Molecular Devices) was used for data acquisition. All whole-cell recordings were conducted at −60 mV and 22 °C.

Laser-Pulse Photolysis Measurements. The laser-pulse photolysis technique was used to measure the channel-opening kinetics (*21*). Briefly, the caged glutamate (*22*) (Invitrogen, Carlsbad, CA) (or free glutamate) with or without the aptamer was dissolved in the extracellular buffer and applied to a cell using a flow device (*19*, *23*). In the laser-pulse photolysis measurement

of channel opening, a single laser pulse at 355 nm with a pulse length of 8 ns was generated from a pulsed Q-switched Nd:YAG laser (Continuum, Santa Clara, CA). The pulse energy varied in the range of 200−800 μJ, measured at the end of an optical fiber (300 μm core diameter) to which the laser was coupled. To calibrate the concentration of photolytically released glutamate, we applied two solutions of free glutamate with known concentrations to the same cell before and after a laser flash (*24*). The current amplitudes obtained from this calibration were compared with the amplitude from the laser measurement with reference to the dose−response relationship (*21*). The analysis of channel-opening kinetic data is described in detail in the Appendix.

Statistical Data Analysis. Unless noted otherwise, each data point, such as $A/A(I)$ or binding data point, was an average of at least three measurements (each of the whole-cell recording data was collected from at least three cells). Uncertainties reported refer to the standard deviation from the mean. The significance of inhibition was evaluated by a one-sample two-tailed Student's t test with the assumption that H_0:$\mu = \mu_0 = 1$, 1 being the theoretical value of no inhibition and indicated by a single blue asterisk ($P \leq 0.05$) or two blue asterisks ($P \leq 0.01$). The significance of the difference between the open-channel and closed-channel conformations was evaluated by a two-sample two-tailed Student's t test with the assumption that H_0:$\mu_1 = \mu_2$ and indicated by a single red asterisk ($P \leq 0.05$) or two red asterisks ($P \leq 0.01$). Origin 7 was used for data analysis and plotting.

RESULTS

Design Strategy for Discovery of Aptamer Targeting the Open-Channel Conformation of AMPA Receptors. In this work, we chose to use the GluA2Q$_{flip}$ AMPA receptor as the target of in vitro selection (Experimental Procedures and Figure S1 of the Supporting Information). GluA2 is one of the four AMPA receptor subunits and can form a homomeric, functional channel by itself, like any other AMPA receptor subunits (*9*). GluA2 is considered a key subunit that mediates excitotoxicity (*25*). The "flip" isoform of GluA2Q or GluA2Q$_{flip}$, generated by alternative splicing, is known to desensitize less rapidly than the "flop" isoform (*5*, *26*). The unedited or Q isoform (i.e., glutamine at the glutamine/arginine or Q/R editing site) is calcium-permeable, whereas the R isoform is not (*27*). An abnormal expression of the Q isoform of GluA2 is linked to neurological disorders such as ALS (*28*).

To make it practically possible to apply an in vitro evolution approach to the identication of aptamers against the open-channel conformation of AMPA receptors, we specifically designed the following experiments. First, we used a saturating agonist concentration to "titrate" the receptor population to maximize the fraction of the open-channel conformation of GluA2Q$_{flip}$. In other words, we wanted to present specifically the open-channel conformation of GluA2Q$_{flip}$ as the target of the selection in anticipation of finding aptamers that would specifically recognize the open-channel conformation. Second, the open-channel conformation lasts no more than a millisecond or so (depending on the glutamate concentration) after glutamate binding (*5*), whereas the binding reaction between the receptor and RNA library requires at least 30 min to reach completion (*19*) (Experimental Procedures and Figure S1 of the Supporting Information). Thus, we had to "trap" the open-channel conformation long enough for the binding reaction. To do so, we decided to choose kainate as the agonist. Kainate is capable of producing a nondesensitizing current response with GluA2 after kainate binds to it, indicative of a persistent existence of the open-channel conformation (*29*). Experimentally, we preincubated the cell membrane containing the GluA2Q$_{flip}$ receptor with 1 mM kainate (i.e., this was a saturating concentration). Third, we used a noncompetitive inhibitor, i.e., GYKI 47409, to elute putative RNAs that might bind to the same site or mutually exclusive sites(s) (Figure S1 of the Supporting Information). GYKI 47409 is a 2,3-benzodiazepine derivative and has an inhibition constant (K_I) of ~3 μM for the open-channel conformation of GluA2Q$_{flip}$ or an ~2-fold higher affinity than it does for the closed-channel conformation (W. Pei and L. Niu, unpublished data). The overall design of our experiments was to specifically identify an aptamer that targeted the open-channel conformation by its binding to a noncompetitive site.

Identification of an RNA Aptamer That Inhibits AMPA Receptors. The GluA2Q$_{flip}$ channels were transiently expressed in HEK-293S cells, and the membrane fragments harboring the entire functional receptors were used for in vitro selection (*19*). To suppress potentially hazardous enrichment of nonspecific RNAs bound to any other "targets", such as lipids, we also conducted the negative selection as in rounds 5, 10, and 13, in a total of 14 selection cycles, in which plain HEK-293 cell membrane lacking only the GluA2Q$_{flip}$ receptors was used to absorb these nonspecific RNAs. In contrast, the positive selection rounds involved the use of GYKI 47409, as mentioned before, for elution of potentially useful RNAs. The eluted RNAs were amplified by RT-PCR, and an enriched RNA library was then transcribed for a new round of selection (Figure S1 of the Supporting Information). After 14 cycles, we identified some enriched sequences (Figure 1A). An enriched sequence was one with at least two copies in the entire sequence pool of 83 clones (i.e., 43 clones from round 12 and 40 clones from round 14). The putative inhibitory property of these enriched sequences was then functionally tested by the use of whole-cell current recording with GluA2Q$_{flip}$ expressed in HEK-293 cells. On the basis of the whole-cell recording results (see representative traces in Figure 1B) or the ratio of the current amplitudes in the absence and presence of an aptamer, $A/A(I)$ (shown in the right column in Figure 1A), we concluded that AG1407, the most enriched sequence, was one of the most potent inhibitors. A further test of AG1407 at the same aptamer concentration but with increasing glutamate concentrations showed that AG1407 inhibited the open-channel conformation of GluA2Q$_{flip}$ (Figure S2 of the Supporting Information).

Identification of the Minimal, Functional Aptamer Sequence. Next we systematically truncated aptamer AG1407 to identify the minimal yet functional sequence. Guided by the secondary structure prediction using Mfold (*30*), we constructed and functionally tested shorter versions of AG1407 (Figure 2A). On the basis of the $A/A(I)$ value (colored red at the bottom of each predicted structure in Figure 2A), we found the 56-nucleotide (nt) version of AG1407, termed AG56, was the functional aptamer with the minimal length of sequence. In contrast, either shortening the three-way junction by deleting the UUGUGA sequence (i.e., the 46 nt RNA), removing the bulge at the U50 position (i.e., 45 nt RNA), or truncating the base-paired stem in the first stem−loop region (i.e., 48 nt RNA) (Figure 2A) resulted in nonfunctional RNAs. Therefore, these structural elements are essential in the folding of AG56 as a functional aptamer. Consequently, we used AG56 as the minimal aptamer for all of the functional characterizations described below.

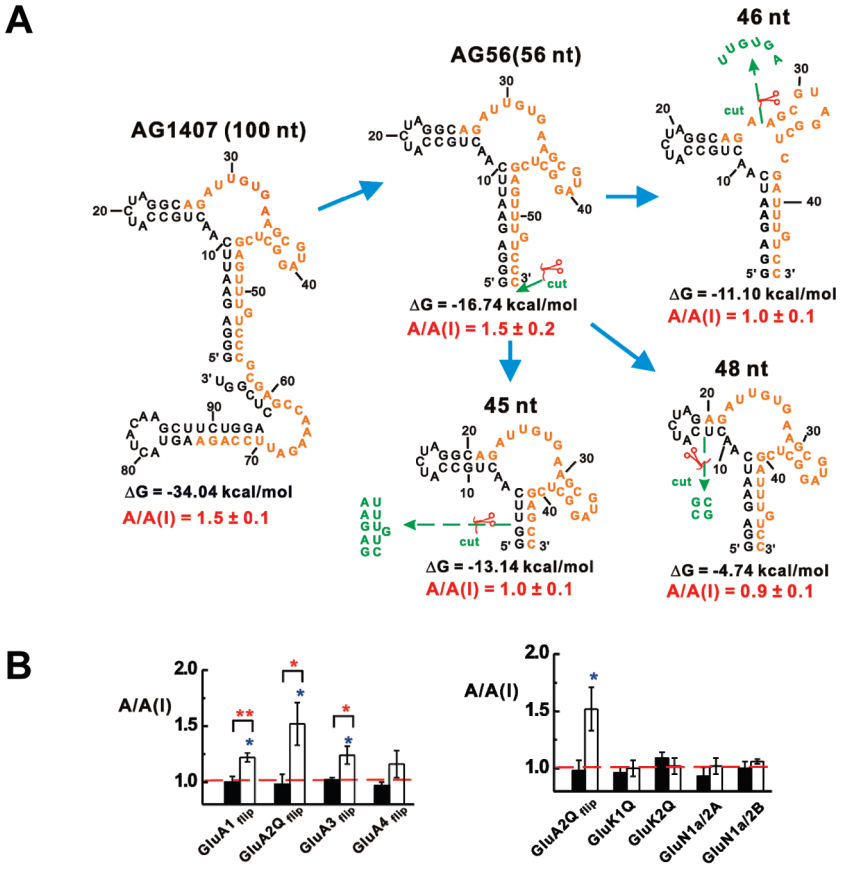

FIGURE 2: Minimal, functional sequence of the aptamer and AMPA receptor subtype selectivity. (A) In the truncation of the sequence of AG1407 to identify the minimal, functional 56 nt sequence or AG56, only the most stable secondary structure of each sequence, with the free energy listed below that structure, was considered, on the basis of the prediction by Mfold. The black and brown colored letters represent the constant and variable sequence regions, respectively. A "scissor" indicates where a particular sequence was cut, and the green letters represent the cutoff nucleotides. The inhibitory function, shown as $A/A(I)$, is listed at the bottom of each truncated structure. (B) By the whole-cell current recording assay, AG56 selectively inhibited the open-channel conformation of all AMPA receptor subunits (left) (see further explanation and statistical analysis in Figure S3 of the Supporting Information), yet AG56 did not affect GluK1Q and GluK2Q, two representative kainate receptor channels or GluN1a/2A and GluN1a/2B NMDA receptor channels. For each of the receptor types tested, the glutamate concentration was chosen to be equivalent to an ~4 and ~95% fraction of the open channels. Specifically, the glutamate concentration was 0.04 mM (for the closed-channel conformation) and 3 mM (for the open-channel conformation) $GluA1_{flip}$, 0.1 and 3 mM for $GluA2Q_{flip}$, $GluA3_{flip}$, and $GluA4_{flip}$, and 0.04 and 3 mM for GluK1Q and GluK2Q, respectively. The glutamate concentrations of 0.02 mM and 0.05 mM were used to assay the aptamer with NMDA receptors.

Functional Characterization of Aptamer AG56 by Whole-Cell Recording. AG56 was functionally characterized in a series of experiments. First, like its predecessor sequence AG1407 (Figure S2 of the Supporting Information), AG56 selectively inhibited the open-channel, but not the closed-channel, conformation of $GluA2Q_{flip}$ (Figure 2B, left). Furthermore AG56 similarly inhibited the open-channel conformation of all other AMPA receptor subunits, i.e., GluA1, -3, and -4, although the inhibitory effect of AG56 on GluA4 was weak (Figure 2B, left, and Figure S3 of the Supporting Information), yet AG56 had no inhibitory effect on any of the closed-channel conformations (Figure 2B, left). AG56 did not affect either the kainate receptor channels (i.e., GluK1 and GluK2) or the NMDA receptor channels (i.e., GluN1a/2A and GluN1a/2B) (Figure 2B, right). It should be noted that GluN1a/2A and GluN1a/2B are two dominant NMDA receptor complexes in vivo (*31*) and neither GluN1a nor GluN2A or GluN2B can form a functional channel by itself (*32*). These results thus suggest that AG56 is an AMPA receptor-subtype-selective inhibitor and targets the open-channel conformations, and AG56 is without any unwanted, cross activity against other glutamate receptor subtypes.

Mechanism of Inhibition of AG56 on $GluA2Q_{flip}$: Homologous Binding Studies. We further elucidated the mechanism of action of AG56 on the $GluA2Q_{flip}$ receptor channel expressed in HEK-293 cells. In this study, we first determined the inhibition constant of AG56 to be $0.95 \pm 0.20\ \mu M$ (the solid line in Figure 3A) for the open-channel conformation of $GluA2Q_{flip}$ at 3 mM glutamate where almost all of the channels were in the open-channel conformation [this was because the EC_{50} value of $GluA2Q_{flip}$ with glutamate was 1.3 mM and the channel-opening probability of $GluA2Q_{flip}$ was near unity (*21*)]. In contrast, AG56 did not inhibit the closed-channel conformation of $GluA2Q_{flip}$, as verified by a series of aptamer concentrations (Figure 3A), but at $100\ \mu M$ glutamate where most of the receptors were in the closed-channel conformation (*21*). This result could be explained by a noncompetitive mechanism by which AG56 bound to a regulatory site or noncompetitive site, and such a site was accessible from both the closed-channel and open-channel states or conformations; however, the interaction of the aptamer with the open-channel conformation resulted in inhibition. Alternatively, this result could be explained by an uncompetitive mechanism, such as an open-channel blockade model, by which AG56 would only inhibit the open-channel conformation, because the uncompetitive site would only be accessible through the open-channel conformation (*33*) (see the two mechanisms in the Appendix). To differentiate these two mechanisms, we first conducted a

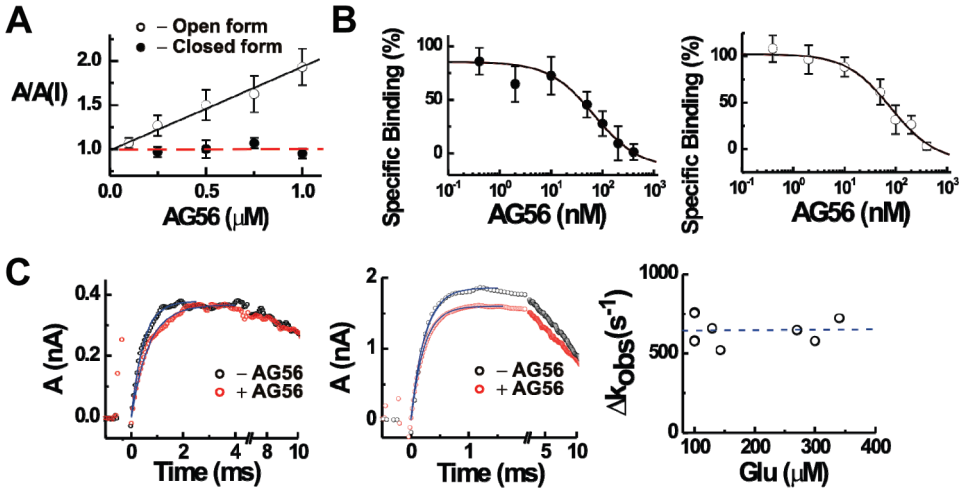

FIGURE 3: Characterization of the inhibition constant, binding affinity, and mechanism of action of AG56 with GluA2Q$_{flip}$ expressed in HEK-293 cells. (A) A whole-cell current recording assay showed that AG56 inhibited the open-channel (measured at 3 mM glutamate), but not the closed-channel (measured at 0.1 mM glutamate), conformation of GluA2Q$_{flip}$ [the dotted line indicates no inhibition or $A/A(I) = 1$]. The inhibition constant, K_I, for the open-channel conformation of GluA2Q$_{flip}$ by AG56 was determined to be 0.95 ± 0.20 μM (i.e., the top solid line). (B) The homologous competition binding of AG56 to the GluA2Q$_{flip}$ receptor was plotted for both the unliganded, closed-channel form (●) and the open-channel form (○). The binding constants, K_d, for binding of AG56 to the closed-channel (left) and open-channel (right) forms of GluA2Q$_{flip}$ was determined to be 68 ± 40 and 80 ± 23 nM, respectively, based on triplicate data sets. The binding constant was calculated using eq 1 in the Appendix. (C) The laser-pulse photolysis measurement of the effect of AG56 on the channel-closing rate constant or k_{cl} (left) and channel-opening rate constant or k_{op} (middle) with GluA2Q$_{flip}$ expressed in HEK-293 cells. Specifically, at a photolytically released glutamate concentration of 100 μM, the k_{obs} value, which reflected k_{cl}, was decreased from 2200 s^{-1} (control or without 0.5 μM AG56, black trace, left) to 1600 s^{-1} (with 0.5 μM AG56, red trace, left). At a photolytically released glutamate concentration of 340 μM, the k_{obs} value, which reflected k_{op} (middle), was 5128 and 4405 s^{-1} in the absence and presence of 0.5 μM AG56, respectively. The difference, however ($\Delta k_{obs} = k_{obs} - k_{obs}' = \Delta k_{cl}$) was invariant even when the glutamate concentration increased (right). Here $\Delta k_{cl} = k_{cl} - k_{cl}'$, where k_{cl}' is the inhibited k_{cl} value and k_{cl} is the channel-closing rate constant without AG56 (see eq 9 in the Appendix). Each data point represents at least one measurement from a single cell where k_{obs} is the control rate constant and k_{obs}' is the rate constant in the presence of 0.5 μM AG56.

homologous competition binding assay (*20*) and observed that AG56 not only bound to the closed-channel conformation (i.e., the unliganded, closed-channel receptor form) but did so with an affinity, i.e., $K_d = 68 \pm 40$ nM (Figure 3B, left), similar to that for the open-channel conformation, i.e., $K_d = 80 \pm 23$ nM (Figure 3B, right). This result was consistent with a noncompetitive mechanism, based on the fact that AG56 was found to bind to the closed-channel conformation in addition to its binding to the open-channel conformation. This result, however, was inconsistent with the uncompetitive mechanism.

Mechanism of Inhibition of AG56 on GluA2Q$_{flip}$: A Laser-Pulse Photolysis Measurement of the Effect of AG56 on the Channel-Opening Rate Process. We further characterized the mechanism of inhibition of AG56 on the channel-opening kinetic process of GluA2Q$_{flip}$. Using a laser-pulse photolysis technique, together with a photolabile precursor of glutamate or caged glutamate, which provided a time resolution of ~30 μs (*22*), we specifically measured the effect of AG56 on both the channel-closing (k_{cl}) and channel-opening (k_{op}) rate constants (*23*) (Figure 3C, left and middle panels, respectively). This experiment enabled us to simultaneously follow not only the rate of channel opening but also the current amplitude, prior to channel desensitization (*23*) (Figure 3C, left and middle panels). The magnitude of k_{cl} reflects the lifetime (τ) of the open channel (i.e., $\tau = 1/k_{cl}$), and the effect of an inhibitor on k_{cl} thus reveals whether it inhibits the open-channel conformation (*23*). In contrast, k_{op} reflects the closed-channel conformation, and the effect on k_{op} reveals whether the inhibitor inhibits the closed-channel conformation (*23*) (see the rate equations and quantitative treatment of the rate data in the Appendix). Experimentally, at a low glutamate concentration (i.e., 100 μM photolytically released glutamate) where k_{cl} was measured (*23*), AG56 inhibited the rate of channel closing, consistent with a noncompetitive mechanism by which it inhibited the open-channel conformation, yet AG56 did not affect the current amplitude (Figure 3C, left panel). This was not surprising because the amplitude observed at this low glutamate concentration (i.e., 100 μM photolytically released glutamate) was dominated by the closed-channel receptor population (notice this was consistent with the amplitude measurement shown as the red dashed line in Figure 3A).

However, when the concentration of glutamate increased and k_{op} became measurable (*23*) (see the Appendix), AG56 did not inhibit k_{op} (Figure 3C, middle and right panels). This result suggested that the inhibition of the rate by AG56 could be completely ascribed to the inhibition of k_{cl} by AG56 such that the difference between the observed rate constant of channel opening or Δk_{obs} in the absence and presence of AG56 but at the same AG56 concentration was invariant in spite of an increasing glutamate concentration (Figure 3C, right panel, and see the mechanistic treatment of the rate data, specifically eq 9 in the Appendix). In other words, the fact that Δk_{obs} remained the same (or Δk_{obs} is constant), verified with a series of increasing glutamate concentrations, was entirely consistent with the prediction by eq 9 (see additional explanation about eq 9 in the Appendix). The lack of an inhibitory effect of AG56 on k_{op} (Figure 3C, middle and right panels) further demonstrated that AG56 did not inhibit the closed-channel conformation.

On the other hand, AG56 reduced the current amplitude at a higher glutamate concentration (see the difference in peak current amplitudes between the red and blue traces in Figure 3C, middle panel; and see an additional trace in Figure S4 of the Supporting Information for a higher-current amplitude inhibition at a higher glutamate and inhibitor concentration). Again, this was expected because the current amplitude at a higher

glutamate concentration began to reflect more the open-channel receptor population. Furthermore, the effect of AG56 on the current amplitude from the rate measurement (Figure 3C, middle panel, and Figure S4 of the Supporting Information) was entirely consistent with the amplitude measurement using a rapid solution flow method (Figure 3A). Taken together, the results from the binding site/affinity assessment (Figure 3B) and the chemical kinetic characterization of the effect of AG56 on both k_{cl} and k_{op} (Figure 3C) as well as the amplitude measurement (Figure 3A) are consistent only with AG56 being a noncompetitive inhibitor selective to the open-channel receptor conformation. Conversely, an uncompetitive mode of action is inconsistent with our data; i.e., AG56 would bind only to the open-channel conformation, but not the closed-channel conformation. A competitive mode of action is also inconsistent with our data; i.e., AG56 would only be effective as an inhibitor at a low ligand concentration and would inhibit k_{op}, but not k_{cl}.

DISCUSSION

In this study, we have described the discovery of a novel inhibitor of AMPA receptors, i.e., aptamer AG56, through an in vitro evolution selection. Using a combination of equilibrium binding and rapid chemical kinetic measurements, we have characterized the mechanism of action of AG56 and have concluded that AG56 inhibits the GluA2Q_{flip} receptor noncompetitively. This conclusion is not surprising, because 2,3-benzodiazepine compounds like the one we used (i.e., GYKI 47409) in the in vitro selection are known as noncompetitive inhibitors. Aptamer AG1407, the predecessor of AG56, which was eluted from the GluA2Q_{flip} receptor by GYKI 47409, was supposedly bound to the same noncompetitive site. In addition, because the open-channel conformation of GluA2Q_{flip}, rather than the closed-channel conformation or a conformation mixture, was exclusively presented as the target of the selection, AG56 was selected, as expected, to specifically recognize and inhibit the open-channel conformation of GluA2Q_{flip}.

The results we have obtained from this study also provide insights into the structural similarity of the open-channel conformations among AMPA receptor subunits. As anticipated, AG56 exhibited the selectivity toward the open-channel conformation of the GluA2 AMPA receptor subunit because GluA2, precisely the open-channel conformation of GluA2, was exclusively presented as the target in the in vitro evolution selection. Interestingly, however, AG56 showed likewise the open-channel conformation selectivity toward the rest of the AMPA receptor subunits, despite the fact that these AMPA receptor subunits had never been presented for evolution selection. A successful in vitro selection of an aptamer from its target is based, at least in part, on the "fitness" or the molecular recognition between the aptamer and its target (*14*). Our result therefore suggests that there should be a considerable structural similarity among AMPA receptor subunits at the level of the open-channel conformation. However, whether there is the same level of structural similarity in the closed-channel conformation among all of the AMPA receptor subunits awaits future studies. This question is important because the answer may well inform what would be a more effective conformation for the development of AMPA receptor subunit-selective inhibitors. Such an inhibitor does not exist today, and developing such an inhibitor will provide us additional ability to control the function of an AMPA receptor one subunit at a time. If our hypothesis is plausible, the open-channel conformation will be a structural platform that can be used for developing nanomolar affinity, noncompetitive inhibitors for the AMPA receptor subtype; however, it might be difficult to find inhibitors selective toward a single AMPA receptor subunit using this platform because of the considerable structural similarity at the level of the open-channel receptor conformation among all AMPA receptors.

The fact that AG56 possesses the unique selectivity toward the open-channel receptor conformation of all AMPA receptors without any inhibitory effect on the closed-channel conformation suggests that this noncompetitive inhibitor may be useful for allowing us to control the AMPA receptor activity in vivo more tightly with minimal, if any, off-target activity. This is because the inhibition of AMPA receptors by AG56 is based on a stronger molecular recognition between AG56 and the specific conformational state of AMPA receptors, rather than a promiscuous recognition of a mixture of functional states. The fact that AG56 targets the open-channel receptor conformation further suggests that the apparent inhibition potency of this noncompetitive aptamer is stronger when the agonist concentration is higher, such as under excitotoxic conditions (see the treatment of amplitude data in the Appendix or a graphic illustration of this notion in Figure 3A). As a comparison, a competitive inhibitor loses its inhibitory potency when the agonist concentration increases (because they compete for the same site) (*19*). Therefore, the discovery of an open-channel conformation-selective inhibitor AG56 not only represents our continuing effort in the development of a "toolbox" of aptamer inhibitors that include competitive (*19*) and now noncompetitive inhibitors but also gives us additional ability to regulate AMPA receptor activities over a wide range of glutamate concentrations.

Our results have demonstrated that using the in vitro evolution method, we can successfully isolate a potent noncompetitive RNA inhibitor from a random sequence library. However, the use of this approach for the evolution of aptamers against a desired target requires target preparation, particularly if the target is a membrane protein. Previously, we reported that glutamate ion channels can be expressed in HEK-293 cells and the membrane fragments harboring total, functional receptors can be prepared for a successful in vitro selection of competitive aptamers (*19*). In this study, we have shown that such a method can also be used successfully in the evolution of noncompetitive inhibitors. In a technically simpler and more conventional approach, a soluble portion of a membrane protein can be used for in vitro selection, and such a water-soluble, partial AMPA receptor construct, which comprises the extracellular binding domain of the AMPA receptors, known as S1S2 protein, has been available (*34*). However, we found previously that GYKI compounds do not bind to this water-soluble S1S2 minireceptor (*23*). Therefore, the target preparation, i.e., the use of the entire functional receptor or GluA2Q_{flip} embedded in a lipid membrane, is a critical component of our success in finding a noncompetitive aptamer, not just the use of an in vitro selection approach.

How are the properties of AG56 compared with those of small molecule inhibitors? First, the high conformational selectivity of AG56 as an AMPA receptor inhibitor is unique. Second, AG56 is more potent than GYKI 47409, the elution agent. In fact, the inhibitory potency of AG56 rivals that of any existing noncompetitive inhibitors documented thus far. Third, small molecule inhibitors of AMPA receptors, prepared by synthetic chemistry, such as quinoxalines, and 2,3-benzodiazepine compounds, generally have limited water solubility, which so often plagues the

clinical usefulness of these compounds (*35*). In contrast, RNA aptamers are naturally water-soluble. Therefore, AG56 represents a water-soluble, highly potent, and highly selective inhibitor of AMPA receptors.

The data we presented here further demonstrate that the open-channel conformation, which lasts less than a few milliseconds in general once glutamate is bound, can be potently and selectively inhibited by druglike molecules in the subnanomolar concentration range. As an RNA molecule, AG56 is readily amenable to structural modifications and large-scale synthesis or transcription for further development into a potent, selective drug candidate and/or biochemical probe targeting AMPA receptors. For instance, AG56 can be chemically modified to become a covalent labeling agent for the mapping of the noncompetitive site of action (*36*). To date, there is no structural information available for any noncompetitive sites on any AMPA receptors. Furthermore, AG56 can be used as the template of chemical modifications to make it ribonuclease-resistant or biostable (*37*). A biostable aptamer can be practically tested in vivo as a viable pharmacological and therapeutic agent for the diagnosis and potential treatment of neurological disorders and diseases. Finally, because AG56 is a water-soluble, noncompetitive inhibitor, our finding represents a major step forward in the exploration of making alternative agents that target excitotoxicity involving excessive AMPA receptor activity.

In conclusion, using an in vitro evolution approach and a random RNA sequence library, we have shown that we can successfully "breed" a new RNA molecule de novo that is capable of noncompetitively inhibiting AMPA receptor activity with nanomolar potency and unique conformational selectivity. Our approach is an alternative to traditional strategies of making noncompetitive inhibitors, for example, by synthetic chemistry. The discovery of AG56 offers promising opportunities to exploit the use of this aptamer both as a mechanistic probe in structure–function studies of AMPA receptors and as a lead molecule in the development of potential therapeutic agents for a number of neurological disorders and diseases. In this context, the unique selectivity of AG56 toward the open-channel receptor conformation of AMPA receptors without any inhibitory effect on the closed-channel conformation offers the possibility of controlling the receptor activity in vivo more tightly with minimal, if any, off-target activity.

APPENDIX

Homologous Competitive Binding Assay. Nonspecific binding was estimated by eq 1. Specific binding was calculated as the difference between the total binding count or counts per minute (cpm) and the estimated nonspecific cpm. Specific binding was also normalized to a percentage on the basis of the CPM value without nonlabeled AG56. Assuming a one-site binding model, the K_d of AG56 bound to GluA2Q$_{flip}$ was estimated by fitting the binding data to eq 1 (*20*)

$$Y = \frac{B_{max}[hot]}{[hot]+[cold]+K_d} + NSB \quad (1)$$

where [hot] and [cold] are the molar concentrations of the unbound labeled or hot AG56 and unlabeled or cold AG56, respectively, and NSB represents nonspecific binding.

Kinetic Data Analysis: Mechanism of Channel Opening. Before we describe the kinetic investigation of the mechanism of inhibition, we first introduce the kinetic characterization of the channel-opening rate process. Using the laser-pulse photolysis technique, we previously determined the rate constants for the GluA2Q$_{flip}$ channel opening (*21*), based on a general mechanism of channel opening shown below.

$$A + L \overset{K_1}{\rightleftharpoons} AL_n \overset{\Phi}{\rightleftharpoons} \underset{(open)}{\overline{AL_n}}$$

where A represents the active form of the receptor, L the ligand, AL_n the closed-channel form, $\overline{AL_n}$ the open-channel form, K_1 the intrinsic dissociation constant of the activating ligand, and Φ the channel-opening equilibrium constant ($\Phi^{-1} = k_{cl}/k_{op}$). On the basis of this mechanism and the assumption that the ligand-binding rate is fast compared to the channel-opening rate, the observed rate constant of channel opening or k_{obs} can be formulated as shown in eq 2.

$$k_{obs} = k_{cl} + k_{op}\left(\frac{L}{K_1 + L}\right)^n \quad (2)$$

$$I_t = I_{max}[1 - \exp(-k_{obs}t)] \quad (3)$$

In eq 2, k_{cl} and k_{op} are the channel-closing and channel-opening rate constants, respectively. n is the number of the ligand molecules that bind to the receptor to open the channel (i.e., $n = 1-4$). I_{max} is the maximum current amplitude, and I_t is the current amplitude at time t. Our previous studies of AMPA receptors, including a mutant AMPA receptor, for their channel-opening kinetic mechanisms led us to conclude that binding of two glutamate molecules per receptor (i.e., $n = 2$) was sufficient to open the channel (*38*). Using the laser-pulse photolysis technique, we previously determined a k_{op} of $(8.0 \pm 0.49) \times 10^4$ s^{-1} and a k_{cl} of $(2.6 \pm 0.20) \times 10^3$ s^{-1} for the channel-opening kinetic constants of the GluA2Q$_{flip}$ receptor (*21*).

Chart 1

Mechanism 1

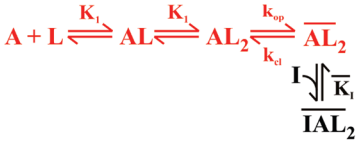

$$k_{obs} = k_{op}\left(\frac{L}{L+K_1}\right)^n + k_{cl}\left(\frac{\overline{K}_I}{\overline{K}_I + I}\right) \quad (4)$$

Mechanism 2

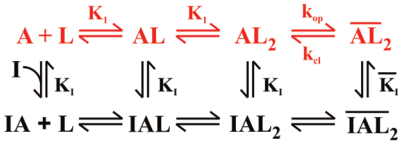

$$k_{obs} = k_{op}\left(\frac{L}{L+K_1}\right)^n\left(\frac{K_I}{K_I + I}\right) + k_{cl}\left(\frac{\overline{K}_I}{\overline{K}_I + I}\right) \quad (5)$$

Kinetic Data Analysis: Mechanism of Inhibition. The mechanism of inhibition was characterized by measuring the effect of AG56 on the channel-opening rate process (*33*, *39*). First, let us assume that an inhibitor binds only to the open-channel conformation and then inhibits it (mechanism 1 in Chart 1, uncompetitive mechanism of inhibition or open-channel blockade). Alternatively, an inhibitor binds to both the closed- and open-channel states through a regulatory site (mechanism 2 in Chart 1, noncompetitive mechanism). The relationship among k_{obs}, the molar concentration of the ligand (glutamate), L, and that of the inhibitor, I, can be written according to the individual mechanism, i.e., eq 4 for mechanism 1 and eq 5 for mechanism 2. In the derivation of these equations, one binding site for the inhibitor per receptor molecule is assumed. At low concentrations of glutamate ($L \ll K_1$), k_{obs} reflects the channel-closing rate constant since the contribution of the k_{op} portion in eq 4 or 5 to the overall rate, k_{obs}, is negligible. Under this condition, the effect of the inhibitor on k_{cl} can be measured (*33*). Specifically, for both mechanisms 1 and 2, the effects of the inhibitor on k_{cl} are the same and can be obtained by using eq 6, which can be derived from either eq 4 or 5. We have previously shown that the k_{obs} value obtained at 100 μM glutamate for GluA2Q$_{flip}$ reflects the k_{cl} (*21*).

$$k_{obs} \approx k_{cl}\left(\frac{\overline{K_I}}{\overline{K_I}+I}\right) \tag{6}$$

In the experiment described in this study, the fact that we observed the inhibition of AG56 on k_{cl} suggested that AG56 inhibited the open-channel conformation of the GluA2Q$_{flip}$ receptor (see Figure 3c, left panel and the legend). Not surprisingly, AG56 was also found to bind to the open-channel conformation (see Figure 3B, right panel).

The effect of an inhibitor on k_{op} is obtained at a high glutamate concentration (where $k_{obs} > k_{cl}$). For mechanism 1 in Chart 1 or the uncompetitive mechanism, the inhibitor does not affect k_{op} (eq 7). The lack of inhibition of the closed-channel conformation, manifested by the lack of an effect on k_{op}, is apparently due to the fact that the inhibitor does not even bind to the closed-channel conformation. In our case here, however, AG56 did bind to the closed-channel conformation, and this result was inconsistent with the uncompetitive mechanism of inhibition, described above.

$$k_{obs} - k_{cl}\left(\frac{\overline{K_I}}{\overline{K_I}+I}\right) = k_{op}\left(\frac{L}{L+K_1}\right)^n \tag{7}$$

For mechanism 2 in Chart 1 or a noncompetitive mechanism of inhibition, the inhibitor will affect k_{op} additionally (eq 8), if $K_I < I$, I being the molar concentration used to measure a K_I value. It should be emphasized that the presence of an inhibitory effect of a noncompetitive inhibitor is due to the fact that the inhibitor must first bind to the closed-channel conformation, as in mechanism 2.

$$k_{obs} - k_{cl}\left(\frac{\overline{K_I}}{\overline{K_I}+I}\right) = k_{op}\left(\frac{L}{L+K_1}\right)^n\left(\frac{K_I}{K_I+I}\right) \tag{8}$$

If, however, the inhibitory effect on the closed-channel conformation is so weak (or $K_I \gg I$), the inhibitor literally no longer inhibits the closed-channel conformation (but still binds to the site). Under this circumstance, the difference in k_{obs} at a defined ligand concentration in the absence (as illustrated in eq 2, which we termed k_{obs}) and presence of a noncompetitive inhibitor (as illustrated in eq 5, which we termed k_{obs}') will be independent of the ligand concentration, as shown in eq 9:

$$\Delta k_{obs} = k_{obs} - k_{obs}' = \left[k_{op}\left(\frac{L}{L+K_1}\right)^n + k_{cl}\right] - \left[k_{op}\left(\frac{L}{L+K_1}\right)^n\left(\frac{K_I}{K_I+I}\right) + k_{cl}\left(\frac{\overline{K_I}}{\overline{K_I}+I}\right)\right]$$

$$\Delta k_{obs} = k_{cl} - k_{cl}\left(\frac{\overline{K_I}}{\overline{K_I}+I}\right) = \Delta k_{cl} \tag{9}$$

In deriving eq 9, we assumed that $K_I \gg I$; thus, the k_{op} portions offset each other. On the basis of eq 9, a plot of $\Delta k_{obs} = k_{obs} - k_{obs}' = \Delta k_{cl}$ versus glutamate concentration would be invariant at the same inhibitor concentration. This was exactly the case with AG56 (see Figure 3C). Our results suggested that AG56 was bound to the closed-channel conformation (Figure 3B, left panel) as a noncompetitive inhibitor, but the binding to the closed-channel conformation of GluA2Q$_{flip}$ was not efficacious or inhibitory.

Amplitude Data Analysis. The amplitude ratio, $A/A(I)$, can be used to independently obtain inhibition constants. The experimental design of using current amplitude to determine the inhibition constant for both the open-channel and closed-channel conformations requires varying concentrations of glutamate, as shown in eqs 10a and 10b. Equations 10a and 10b are derived on the basis of one inhibitor binding to the receptor. $K_{I,app}$ is the apparent inhibition constant for the inhibitor; $(\overline{AL_2})$ represents the fraction of the open-channel form with n = 2; other terms have been defined previously.

$$\frac{A}{A(I)} = 1 + I\,\frac{(\overline{AL_2})}{K_{I,app}} \tag{10a}$$

$$(\overline{AL_2}) = \frac{\overline{AL_2}}{A + AL + AL_2 + \overline{AL_2}} = \frac{L^2}{L^2(1+\Phi) + 2K_1L\Phi + K_1{}^2\Phi} \tag{10b}$$

Specifically in our experiments, at low glutamate concentrations (i.e., $L \ll K_1$), the majority of the receptors in a receptor population were in the closed-channel conformation, since we measured the macroscopic current response or the response from an ensemble of receptors expressed in a single HEK-293 cell. Under this condition, the inhibition constant for the closed-channel conformation was determined from the ratio of the amplitude according to eqs 10a and 10b. Likewise, at a saturating ligand concentration (i.e., $L \gg K_1$), the majority of the receptors were in the open-channel state. Consequently, the inhibition constant associated with the open-channel conformation was measured. The basis of using the two ligand concentrations that corresponded to ~4 and ~96% fractions of the open-channel receptor form (*21*) to determine the corresponding inhibition constant was a putative difference in inhibition constant between the closed-channel and open-channel conformation. At those low and high ligand concentrations (*21*), the apparent inhibition constants obtained were considered pertinent to the closed-channel and open-channel conformations, respectively (*23*).

ACKNOWLEDGMENT

We thank Hua Shi for the original RNA library, Geoffrey Swanson for the GluK1 kainate receptor plasmid, John Woodward for NMDA receptor plasmids, and Sandor Solyom for the GYKI compound.

SUPPORTING INFORMATION AVAILABLE

Schematic diagram showing SELEX; additional data showing that AG1407 at full length inhibited $GluA2Q_{flip}$ receptor more strongly as the glutamate concentration increased; additional data showing that although weak, AG56 inhibited the open-channel conformation of the GluA4 receptor subunit; and an additional trace showing that AG56 did not additionally inhibit the k_{obs} more than it did the k_{cl} (yet this trace had a higher percentage of whole-cell current reduction). This material is available free of charge via the Internet at http://pubs.acs.org.

REFERENCES

1. Henzler-Wildman, K. A., Lei, M., Thai, V., Kerns, S. J., Karplus, M., and Kern, D. (2007) A hierarchy of timescales in protein dynamics is linked to enzyme catalysis. *Nature 450*, 913–916.
2. Frederick, K. K., Marlow, M. S., Valentine, K. G., and Wand, A. J. (2007) Conformational entropy in molecular recognition by proteins. *Nature 448*, 325–329.
3. Wolan, D. W., Zorn, J. A., Gray, D. C., and Wells, J. A. (2009) Small-molecule activators of a proenzyme. *Science 326*, 853–858.
4. Lerner, R. A., Benkovic, S. J., and Schultz, P. G. (1991) At the crossroads of chemistry and immunology: Catalytic antibodies. *Science 252*, 659–667.
5. Pei, W., Huang, Z., Wang, C., Han, Y., Park, J. S., and Niu, L. (2009) Flip and flop: A molecular determinant for AMPA receptor channel opening. *Biochemistry 48*, 3767–3777.
6. Trussell, L. O., and Fischbach, G. D. (1989) Glutamate receptor desensitization and its role in synaptic transmission. *Neuron 3*, 209–218.
7. Hollmann, M., and Heinemann, S. (1994) Cloned glutamate receptors. *Annu. Rev. Neurosci. 17*, 31–108.
8. Seeburg, P. H. (1993) The TINS/TiPS Lecture. The molecular biology of mammalian glutamate receptor channels. *Trends Neurosci. 16*, 359–365.
9. Dingledine, R., Borges, K., Bowie, D., and Traynelis, S. F. (1999) The glutamate receptor ion channels. *Pharmacol. Rev. 51*, 7–61.
10. Palmer, C. L., Cotton, L., and Henley, J. M. (2005) The molecular pharmacology and cell biology of α-amino-3-hydroxy-5-methyl-4-isoxazolepropionic acid receptors. *Pharmacol. Rev. 57*, 253–277.
11. Heath, P. R., and Shaw, P. J. (2002) Update on the glutamatergic neurotransmitter system and the role of excitotoxicity in amyotrophic lateral sclerosis. *Muscle Nerve 26*, 438–458.
12. Tuerk, C., and Gold, L. (1990) Systematic evolution of ligands by exponential enrichment: RNA ligands to bacteriophage T4 DNA polymerase. *Science 249*, 505–510.
13. Ellington, A. D., and Szostak, J. W. (1990) In vitro selection of RNA molecules that bind specific ligands. *Nature 346*, 818–822.
14. Wilson, D. S., and Szostak, J. W. (1999) In vitro selection of functional nucleic acids. *Annu. Rev. Biochem. 68*, 611–647.
15. Marcaurelle, L. A., and Johannes, C. W. (2008) Application of natural product-inspired diversity-oriented synthesis to drug discovery. *Prog. Drug Res. 66* (187), 189–216.
16. Hruby, V. J. (2009) Organic chemistry and biology: Chemical biology through the eyes of collaboration. *J. Org. Chem. 74*, 9245–9264.
17. Nimjee, S. M., Rusconi, C. P., and Sullenger, B. A. (2005) Aptamers: An emerging class of therapeutics. *Annu. Rev. Med. 56*, 555–583.
18. Huang, Z., Li, G., Pei, W., Sosa, L. A., and Niu, L. (2005) Enhancing protein expression in single HEK 293 cells. *J. Neurosci. Methods 142*, 159–166.
19. Huang, Z., Pei, W., Jayaseelan, S., Shi, H., and Niu, L. (2007) RNA aptamers selected against the GluR2 glutamate receptor channel. *Biochemistry 46*, 12648–12655.
20. Swillens, S. (1995) Interpretation of binding curves obtained with high receptor concentrations: Practical aid for computer analysis. *Mol. Pharmacol. 47*, 1197–1203.
21. Li, G., Pei, W., and Niu, L. (2003) Channel-opening kinetics of $GluR2Q_{flip}$ AMPA receptor: A laser-pulse photolysis study. *Biochemistry 42*, 12358–12366.
22. Wieboldt, R., Gee, K. R., Niu, L., Ramesh, D., Carpenter, B. K., and Hess, G. P. (1994) Photolabile precursors of glutamate: Synthesis, photochemical properties, and activation of glutamate receptors on a microsecond time scale. *Proc. Natl. Acad. Sci. U.S.A. 91*, 8752–8756.
23. Ritz, M., Micale, N., Grasso, S., and Niu, L. (2008) Mechanism of inhibition of the GluR2 AMPA receptor channel opening by 2,3-benzodiazepine derivatives. *Biochemistry 47*, 1061–1069.
24. Li, G., and Niu, L. (2004) How fast does the GluR1Qflip channel open? *J. Biol. Chem. 279*, 3990–3997.
25. Tanaka, H., Grooms, S. Y., Bennett, M. V., and Zukin, R. S. (2000) The AMPAR subunit GluR2: Still front and center-stage. *Brain Res. 886*, 190–207.
26. Mosbacher, J., Schoepfer, R., Monyer, H., Burnashev, N., Seeburg, P. H., and Ruppersberg, J. P. (1994) A molecular determinant for submillisecond desensitization in glutamate receptors. *Science 266*, 1059–1062.
27. Lomeli, H., Mosbacher, J., Melcher, T., Hoger, T., Geiger, J. R., Kuner, T., Monyer, H., Higuchi, M., Bach, A., and Seeburg, P. H. (1994) Control of kinetic properties of AMPA receptor channels by nuclear RNA editing. *Science 266*, 1709–1713.
28. Kwak, S., and Kawahara, Y. (2005) Deficient RNA editing of GluR2 and neuronal death in amyotropic lateral sclerosis. *J. Mol. Med. 83*, 110–120.
29. Patneau, D. K., Vyklicky, L., Jr., and Mayer, M. L. (1993) Hippocampal neurons exhibit cyclothiazide-sensitive rapidly desensitizing responses to kainate. *J. Neurosci. 13*, 3496–3509.
30. Zuker, M. (2003) Mfold web server for nucleic acid folding and hybridization prediction. *Nucleic Acids Res. 31*, 3406–3415.
31. Wenthold, R. J., Petralia, R. S., Blahos, J., II, and Niedzielski, A. S. (1996) Evidence for multiple AMPA receptor complexes in hippocampal CA1/CA2 neurons. *J. Neurosci. 16*, 1982–1989.
32. Erreger, K., Dravid, S. M., Banke, T. G., Wyllie, D. J., and Traynelis, S. F. (2005) Subunit-specific gating controls rat NR1/NR2A and NR1/NR2B NMDA channel kinetics and synaptic signalling profiles. *J. Physiol. 563*, 345–358.
33. Niu, L., and Hess, G. P. (1993) An acetylcholine receptor regulatory site in BC3H1 cells: Characterized by laser-pulse photolysis in the microsecond-to-millisecond time region. *Biochemistry 32*, 3831–3835.
34. Kuusinen, A., Arvola, M., and Keinanen, K. (1995) Molecular dissection of the agonist binding site of an AMPA receptor. *EMBO J. 14*, 6327–6332.
35. Weiser, T. (2005) AMPA receptor antagonists for the treatment of stroke. *Curr. Drug Targets: CNS Neurol. Disord. 4*, 153–159.
36. Breaker, R. R. (2004) Natural and engineered nucleic acids as tools to explore biology. *Nature 432*, 838–845.
37. Brody, E. N., and Gold, L. (2000) Aptamers as therapeutic and diagnostic agents. *J. Biotechnol. 74*, 5–13.
38. Pei, W., Ritz, M., McCarthy, M., Huang, Z., and Niu, L. (2007) Receptor occupancy and channel-opening kinetics: A study of GLUR1 L497Y AMPA receptor. *J. Biol. Chem. 282*, 22731–22736.
39. Niu, L., Abood, L. G., and Hess, G. P. (1995) Cocaine: Mechanism of inhibition of a muscle acetylcholine receptor studied by a laser-pulse photolysis technique. *Proc. Natl. Acad. Sci. U.S.A. 92*, 12008–12012.